Fractional order control for bidirectional converter operating in a DC microgrid

Control de orden fraccionario para un convertidor bidireccional operando en un microrred DC

César Trujillo-Rodríguez[1]
Johan Sánchez-Choachí[2]
Giovanni Baquero-Rozo[3]

[1] Universidad Distrital Francisco José de Caldas (Colombia). Correo electrónico: cltrujillo@udistrital.edu.co; orcid: http://orcid.org/0000-0002-0985-1472

[2] Universidad Distrital Francisco José de Caldas (Colombia). Correo electrónico: jossanchezc@correo.udistrital.edu.co; orcid: http://orcid.org/0000-0002-1945-5975

[3] Universidad Nacional de Colombia (Colombia). Correo electrónico: gabaqueror@unal.edu.co; orcid: http://orcid.org/0000-0003-3789-2244

Recibido: 11-09-2019 Aceptado: 16-12-2019

Cómo citar: Trujillo-Rodríguez, César; Sánchez-Choachí, Johan; Baquero-Rozo, Giovanni (2020). Fractional order control for bidirectional converter operating in a DC microgrid. *Informador Técnico, 84*(1), 67-77.
https://doi.org/10.23850/22565035.2387

Abstract

This paper presents the control design of a bidirectional converter used to support a DC microgrid. The chosen topology for this purpose is the bidirectional buck-boost converter, for which its mathematical model is obtained. Next, a brief introduction of fractional order control is presented and the structure of a fractional order PID controller is shown. The tuning process of this controller is obtained by means of an arithmetic method whose parameters are set to control the bidirectional converter. In order to evaluate the performance of the converter and its fractional-order controller, this is simulated under different situations that represent different operating conditions, such as changes in battery voltage levels, climatic conditions, and uncertainty in the parameters. The simulation results of this controller are analyzed and compared with a classical PID. Finally, the conclusions are presented.

Keywords: bidirectional converter; DC microgrid; fractional-order control; robustness.

Resumen

Este artículo presenta el diseño del control de un convertidor bidireccional el cual es usado para brindar soporte eléctrico a una microrred DC. La topología elegida para este propósito es un convertidor bidireccional Buck-boost, para el cual se obtiene el modelo matemático. A continuación se presenta una breve introducción al concepto de control de orden fraccionario, en donde se muestra la estructura de un PID de orden fraccionario. Luego se muestra el proceso de sintonización de los parámetros de este controlador usando un método aritmético. Con el objetivo de evaluar el desempeño del convertidor y su controlador de orden fraccionario, se simula bajo diferentes situaciones que representan distintas condiciones de operación, tales como cambios en los niveles de tensión de la batería, condiciones climáticas e incertidumbre en los parámetros. Se analizan y comparan los resultados de simulación del controlador con los obtenidos de un PID clásico. Finalmente, se presentan las conclusiones.

Palabras clave: convertidor bidireccional, control de orden fraccionario, microrred DC, robustez.

1. Introduction

Currently, distributed generation systems (DG) such as wind and PV farms, have received great attention worldwide as an effective solution for problems such as the increasing of the load factor, which could reach the current limit capacity of power systems (Lee; Kang; Park, 2016). In addition, DGs offer great technical and economic benefits, but the unification of several electric features into a single unit is needed (Perez; Kagan, 2016). This kind of unit is called microgrids. These systems are electric power grids confined locally and whose purpose is to integrate alternative energy sources with the loads, making stable and efficient systems (Krishnamurthy; Kwasinski, 2016). Until now, AC microgrids are the most common ones, however, low and medium DC power distribution systems, used in telecommunication systems and electric vehicle (EV) charging infrastructures as shown in Figure 1, are widely used because they do not have problems of synchronism and harmonic distortion (Sirsi; Prasad; Sonawane; Lokhande, 2016). In the study of Manandhar; Ukil and Jonathan (2015) is presented the DC and AC systems modeling including their power converters, power cable losses and loads. Then, these systems are simulated, finding efficiency of 78.24 % and 84.6 % for low voltage AC and DC systems respectively. This shows that the efficiency of the DC systems is higher than the AC systems under some conditions (Lee *et al.*, 2016), which makes DC grids more efficient systems.

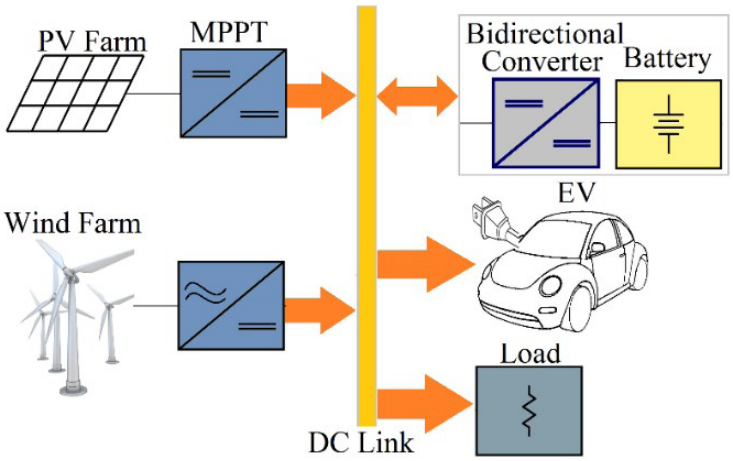

Figure 1. General microgrid scheme
Source: authors.

A lot of DC microgrids include photovoltaic and wind power sources, which dependent on weather conditions, resulting in power fluctuations that affect the power flow between the sources and the load (Alam; Muttaqi; Sutanto, 2013; Takagi *et al.*, 2013; Tamura, 2016) and the hybrid energy storage system (HESS). Additionally, changes in load and generation levels lead to voltage disturbances in the DC link. These changes affect the power quality managed by the microgrid and produce malfunction of devices and loads connected to it. For these reasons, it is necessary to include an energy storage system with bidirectional DC-DC converters to ensure energy storage when there is a surplus or delivery it when the sources cannot give enough energy to the loads. However, these converters must meet some requirements, and one of them is high efficiency. Another requirement is to respond quickly to any voltage level fluctuation on the DC link and any other disturbance (Tummuru; Mishra; Srinivas, 2015). There are several topologies such as dual active bridge and bidirectional flyback, which offer galvanic isolation and high energy density. Another group of topologies is the non-isolated converters, where the most common ones are: zeta, zepic, cuck/cuck, and buck-boost topologies. Nevertheless, this last group does not have high-frequency transformers and does not offer high energy density. Moreover, this converter has low voltage gain, although some modified versions can be found in academic literature. One example of this is the buck-boost modified converter propose in Banaei and Sani (2018), which structure contains only one switch and, unlike many other DC converters, has low stress across the only switch. Notwithstanding, owing to this topology is not bidirectional, it is needed to connect the two voltage levels by two converters, one for each power flow direction.

One of the most used controllers is the PID controller owing to its simplicity and good performance. However, other controllers such as a fuzzy logic controller, adaptive or predictive controller can offer better performance but have a more complex structure. Thus, it is necessary to compare performance with complexity and then to choose the better option. Some works have tackled this issue from different perspectives, which is one of them the passivity control used in Montoya-Giraldo; Garcés-Ruiz; Ortega-Velázquez; Espinosa-Pérez (2018). However, passivity control in itself is no robust which means it is sensible to perturbations in the system. For this, additional strategies have to be added to control passivity to allow an acceptable performance of the converter in real conditions. In Sanchez-Choachí (2019) an adaptative strategy is used to improve the passivity control performance, and additionally, instead of controlling the battery current as in Montoya *et al.*, (2018), the output voltage is regulated indirectly to keep the DC voltage at the reference level.

Fractional order control (FOC) is one of the control techniques whose structure is similar to PID's, but it has additional parameters. Nevertheless, it is simpler than others like compensation nets, fuzzy controllers, among others. Other significant advantages are higher robustness level and ease of design. For this reason, this kind of controllers is used in mechanical, automatic, thermal and pressure areas (Kanagaraj; Al-Dhaifalla; Nisar, 2017). Until now, there are three fractional order control generations, where the first-generation control is the simplest, and it is the one is used in this paper. In some studies like Lei; Xiong; Lei (2017), FOCs are applied to different converters; however, none of them are applied to a bidirectional converter.

This paper presents the modeling of a bidirectional buck-boost converter and develops its fractional order controller (FOC). The tuning detailed process of this FOC is shown with all its numeric parameters. Then, this FOC is approximated using linear filters. Next, the converter and the designed FOC are simulated for different operating conditions. These simulation results are compared with a classical PID controller. Finally, the conclusions about the design process and the outcomes of this work are shown.

2. Converter modeling

As was mentioned previously, there are a lot of conversion topologies that raise or reduce the voltage level between its output terminals. One of these topologies is the buck-boost converter, shown in Figure 2. In this figure, i_p is the current generated by the microgrid sources, E is the battery voltage, v_c is the capacitor voltage which is the DC link voltage too, i_L is the current across the inductor (L) and R_{DC} is the grid load. The current (i_p) represents the grid sources, whose current value can change in order to simulate different weather conditions. Additionally, Rs are included to represent generation and conversion losses.

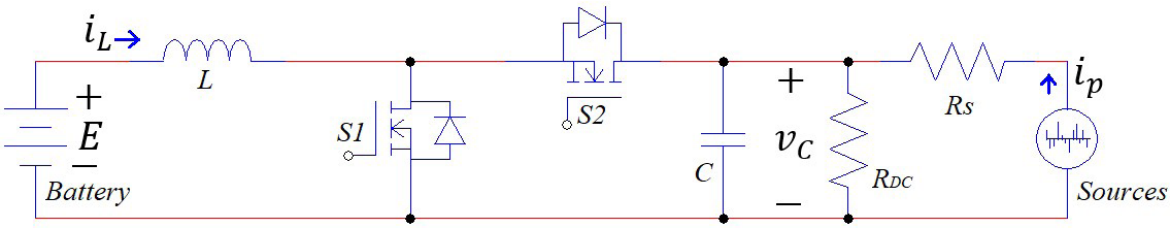

Figure 2. Bidirectional Buck-boost topology
Source: Authors.

This topology is typically used for low voltage applications due to its low ratio conversion. However, this converter can be used for high voltage applications using it to build a modular multilevel converter by means of using methodologies as proposed in Kung and Kish (2018). This methodology apportions the semiconductor devices into switching cells (with $n \geq 2$), then using a harmonic power balance concept, the direction of average ac power flow is identified. Once this is done, the original cells are replaced with new switching cells comprised of series/cascaded subsystems that allow the required ac power flow. Finally, the fundamental frequency ac currents are canceled by interleaving multiple strings subsystems. In fact, the aforementioned methodology is used on the buck-boost converter yielding a new topology.

The buck-boost bidirectional power converter operates as a boost converter if the power flows from the battery to the DC link and operates as a buck converter if the current goes from the DC link to the battery. For this reason, v_c voltage must be larger than E. Another restriction of this converter is that $S1$ and $S2$ diodes have to be fast recovery to avoid working failures since the $S2$ diode works when the current goes from E to v_c and $S1$ diode operates in the opposite case. Therefore, slow current or voltage transitions affect the converter efficiency and behavior (Chun; Rui; Hongwen; Xiaofeng; Weixiang, 2016).

The mathematical model of this converter is developed by assuming that the system is operating in a stationary point so v_c has a constant value. Moreover, the voltage drop in the diode (v_d) is included to consider electrical losses in the model. Then, the average model of the buck-boost converter is obtained by evaluating the state of $S1$ and $S2$ and remembering that these states are opposite, which means that if $S1$ is open then $S2$ is closed and vice versa. This mathematical model is shown in equation (1), where u is the period percentage in which $S1$ is closed. This variable is known as the duty cycle.

$$L\frac{di_L}{dt} = E - v_C(1-u) - v_d(1-u)$$
$$C\frac{dv_C}{dt} = i_L(1-u) - i_p - \frac{v_C}{R_{DC}} \quad (1)$$

3. Fractional order control

This kind of control is similar to traditional linear controllers, but instead of using traditional calculus, it uses the fractional order calculus. This calculus, developed by Riemann and Liouville, is a generalization of the differentiation concept, where its order can be a real number or even a complex number. The differentiation operator can be represented by the operator D_a which is defined by the equation (2) when it operates over a generic function $f(t)$. In this equation, $a \in R$ is the fractional-order and it is in the numeric interval $(n, n+1)$, being n the closest integer to a (but $n < a$) (but) and is the gamma function.

$$D_\propto = \frac{1}{\Gamma(n-\propto)}\frac{d^n}{dt^n}\int_a^t \frac{f(\tau)}{(t-\tau)^{\propto-n+1}}d\tau \quad (2)$$

The equation (2) is known as Cauchy's formula. If initial conditions are assumed zero, this formula represents the $f(t)$ repeated integral of order n by means of a unique integral pondered by the gamma function. With this representation, the integration and derivative concept can be generalized and take a fractional order. Initially, this concept only had mathematical worth because its physical meaning was not considered since physical laws are understood from integer order calculus. Nevertheless, recent research has shown fractional-order calculus is useful to model complex liquids, thermal processes, mechanical systems, signal and image processing and materials (Sun; Zhang; Baleanu, Chen; Chen, 2018).

Using equation (2) to incorporate fractional order calculus in control theory, some common tools can be improved. For instance, in the Laplace domain, the generalized structure of a fractional order PID (FOPID) is given by the equation (3), where k_p, k_I and k_D are the proportional, integral and derivative gains respectively and are the fractional orders of the derivative and integration operator. These two new parameters, that PID controllers do not have, allow us to control more system response features that could improve the plant's behavior, maintaining a simple control structure.

$$C_{FO} = k_p + \frac{k_I}{S^\propto} + k_D S^\beta = \frac{k_p S^\propto + k_I + k_D S^{\beta+\propto}}{S^\propto} \quad (3)$$

Unfortunately, fractional order controllers have infinite dimensions, so, an approximation using linear filters is needed to implement an FOC. This approximation can be developed by different methods; however, the simplest one is the CRONE (Non-Integer Order Robust Control) approximation. The first step of this approximation is restricting the frequency band on which the designed FOC operation is required (from ω_h to ω_b). Next, poles and zeros corner frequencies (ω_k and respectively) have to be distributed in order to emulate the FOC behavior. This approximation is represented by equation (4) and it is the product of *N* poles and *N* zeros, where the number of linear filters (*N*) is chosen as is shown by equation (5).

$$D_a^{\alpha}(s) = C\left(\frac{1+\frac{S}{\omega_h}}{1+\frac{S}{\omega_b}}\right)^{\alpha} \approx C\frac{\prod_{k=1}^{N}\left(1+\frac{S}{\widetilde{\omega_k}}\right)}{\prod_{k=1}^{N}\left(1+\frac{S}{\omega_k}\right)} \tag{4}$$

The corner frequencies ω_k and $\tilde{\omega}_k$ must be distributed recursively to obtain the required frequency behavior and to approximate the FOC performance. However, there is a numeric method used to determinate each ω_k and $\tilde{\omega}_k$ This method is an iterative process described by the equation (5), where once the first converter frequency () is defined, the other frequencies are established.

$$\begin{aligned} \widetilde{\omega_1} &= \alpha\omega_1 & \omega_1 &= \mu^{0,5}\omega_b \\ \widetilde{\omega_{k+1}} &= \alpha\mu\widetilde{\omega_k} & \omega_{k+1} &= \alpha\mu\omega_k \\ \mu &= \frac{\log(\alpha)}{\log(\alpha\mu)} & N &= \frac{\log(\omega_h/\omega_b)}{\log(\alpha\mu)} \end{aligned} \tag{5}$$

The number of linear filters (*N*) has to be approximated the closest integer, but less than the indicated value by equation (5). However, because of the infinite dimension of the FO controller, the larger is, the better is the approximation to FO controller behavior. So, if increasing the number of linear filters is desired, ω_1 has to be closer to ω_b .

4. Control design

It is possible to find several tuning methods such as Grunwald-Letnikoff or Matsuda approximation, but this paper uses the analytic method described below. This method is based on four parameters: phase margin, φ_m, gain margin, g_m, gain crossover frequency, ω_c, phase crossover frequency, ω_p, and phase flatness. According to the system needs, the above parameters are set and by using the equations (6), the k_P, k_I, k_D, and β values are established.

$$\begin{aligned} k_p + \frac{k_I e^{-j\alpha\pi/2}}{{\omega_c}^{\alpha}} + k_d {\omega_c}^{\beta} e^{j\beta\pi/2} &= \frac{e^{j(-\pi+\varphi_m-Ang(G(j\omega_c)))}}{|G(j\omega_c)|} \\ k_p + \frac{k_I e^{-j\alpha\pi/2}}{{\omega_p}^{\alpha}} + k_d {\omega_p}^{\beta} e^{j\beta\pi/2} &= \frac{e^{j(-\pi-Ang(G(j\omega_p)))}}{g_m|G(j\omega_p)|} \\ \left.\frac{d(C_{FO}G)}{d\omega}\right|_{\omega_s} &= 0 \end{aligned} \tag{6}$$

By linearizing the equation (1) around its equilibrium point, the equation (7) is developed. This equation is the converter transfer function that relates the duty cycle (u) to the output voltage, being this the controlled variable. V_{Ce} is the equilibrium point of the output voltage, which is 220 V in this case, i_{Le} is the equilibrium value of the current across the coil, u_e is the nominal value of the duty cycle to get an output voltage equal to 220 V from input voltage E =120 V.

$$G(s) = \frac{v_C(s)}{u(s)} = \frac{V_{Ce}(1-u_e)-s(i_{Le}L)}{s^2LC+S\frac{L}{R_{DC}}+(1-u_e)^2} \qquad (7)$$

The output capacitor (C) is a key element in the converter and as is evident from the equation (7), the transfer function of this system is sensitive to C changes. In order to show this converter sensitivity, Figure 3 presents the bode plot of equation (7) for three different values of C, namely, 80 µF, 100 µF and, 120 µF. As can be seen on the right side of this figure, around f_C (gain crossover frequency), the converter phase is almost constant whereas its magnitude is uncertain, which makes the converter has different bandwidths.

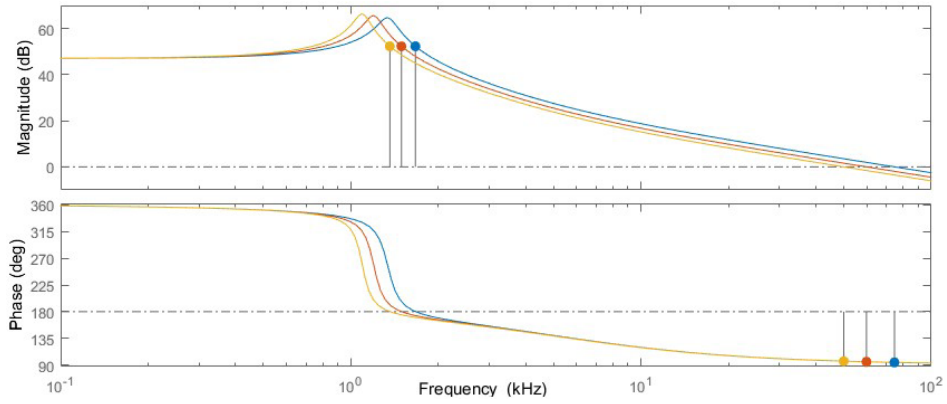

Figure 3. Converter Bode plot for different capacitance values
Source: authors.

In this figure, the red curve is the transfer function of the nominal plant (C=*100 µF*). This feature makes the converter a suitable system for first-generation CRONE control since despite its bandwidth varies, its phase keeps almost constant in the same frequency range. This is the reason why only capacitance changes are considered since if inductance changes are considered, the system's Bode plot shows bandwidth variations as well as phase variations around the frequency of interest.

Subsequently, the converter is designed to operate in continuous conduction mode (5 % current ripple, 2 % output voltage and power equal to 4.4 kW). Then, using the transfer function (7) and solving the equation (6), the FOPID is tuned. Table 1 has the converter and FOPID parameters obtained after the design process described above. In this table, the capacitance is set at the nominal value, however, this value varies by 20 % in the simulation.

The converter, its FO controller approximation and the general scheme of connections are shown in Figure 4. In this figure, the error signal (e) is the result of the difference between the output and reference voltage, and then this signal is applied to the FOPID comprised by the transfer functions of the equation (4). The FOPID generates the duty cycle and then given it to the converter.

Table 1.
Converter and controller parameters

Parameter	Value
L[μH]	50
C[μF]	100
R[Ω]	11
k_p	0.11
k_I	0.00023
k_D	0.044
α	1.2
β	0.6
$\varphi_{m[°]}$	60
$g_{m[dB]}$	18
E[V]	120
v_c [V]	220
N	3

Source: authors.

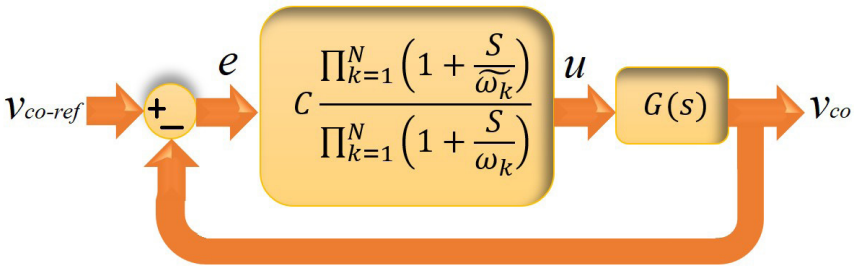

Figure 4. FOPID Control scheme
Source: authors.

5. Simulation results

Once the converter and the controllers have been designed, the simulation of the bidirectional converter is developed by using PSIM software with a switching frequency equal to 25 kHz. In this simulation, the FOC is implemented using the approximation of the equation (4) with $N = 3$ given by equation (5). In the first simulation situation, the microgrid sources are disconnected (thus $i_p = 0$ and the power is provided by the battery) and the reference voltage (equal to DC link voltage) takes three different values, namely, 200 V, 220 V, and 240 V.

As is shown in Figure 5, both FOC and PID controller, have fast response without overshoots. However, FOC has a settling time of 0.006 s whereas PID settling time is equal to 0.011 s.

In the second case, battery voltage changes as a consequence of its state of charge variation. This situation is simulated changing the *E* voltage, taking values within 100 V and 140 V, which means a tolerance around 17 %. This tolerance of the battery voltage is from its state of charge varying from 15 % to 100 %, the percentage recommended for lead-acid batteries. Additionally, in this case, in order to evaluate the converter robustness level, its capacitance value was changed to 80 μF.

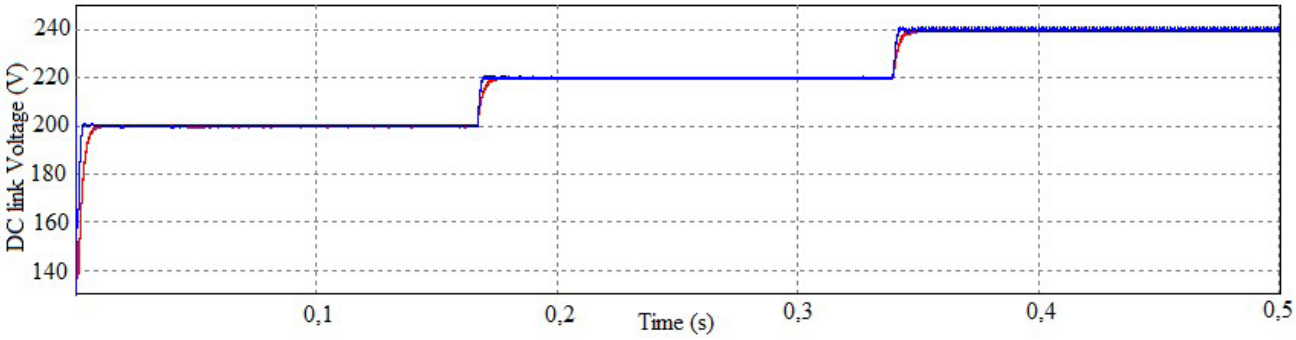

Figure 5. Converter output voltage with PID (red) and with FOC (blue) for different references
Source: authors.

Figure 6 shows the system response with the changes described previously. In this figure, each battery voltage transition takes 1 ms and the settling time of the system is around 24 ms. For these battery voltage changes, the bidirectional converter response has an overshoot without oscillations that fades away after some time. Furthermore, if the output voltage of Figure 6 is compared with Figure 5, it is evident that for figure 6 the ripple voltage is larger. This is because the capacitor has a lower value; however, the converter stability is maintained.

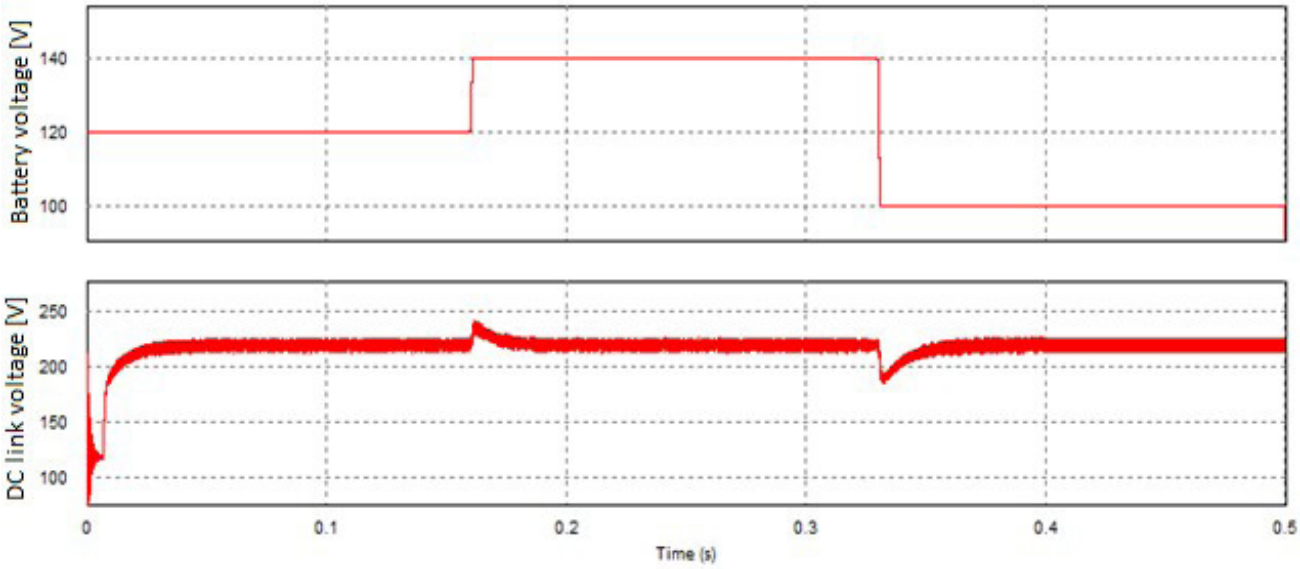

Figure 6. Battery voltage (up) and DC link voltage (down)
Source: authors.

For the third simulation situation, the reference voltage of the converter remains constant at 220 V while the current of the sources varies from 0 A to 20 A. This aims to simulate different weather conditions like solar radiation and wind variations that produce power changes. Figure 7 presents the results of this situation. In this figure the converter load and source currents are shown for 5 different generation levels. As can be seen from Figure 7, the sum of these currents is equal to zero, while the DC link voltage is constant. That means the energy surplus generated by the sources of the microgrid is stored in the battery, whereas when the sources cannot generate enough energy to supply the microgrid loads, the bidirectional power system releases the stored energy previously to give the necessary power to the loads and maintain the DC link voltage constant. This demonstrates the FOPID capacity to operate in a wide uncertainty range while the desired converter behavior is maintained and the power quality is preserved.

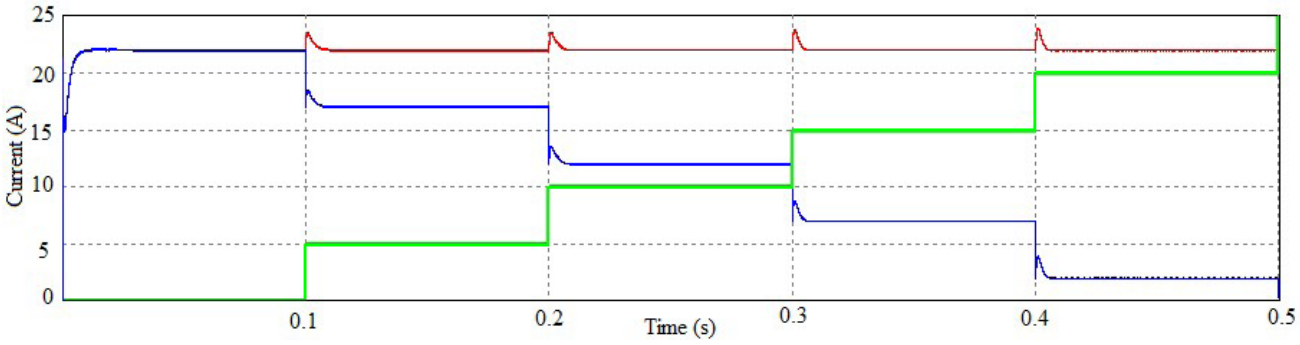

Figure 7. Load (red), ESS (blue) and sources (green) currents for different generation levels
Source: authors.

6. Conclusions

In this paper a bidirectional buck-boost converter and a FOC was designed and simulated. The FOC used in this paper is a FOPID, which has a similar structure to classical PIDs. However, as is shown in this paper, FOC has two more parameters that allow improving the converter behavior, giving fast response to reference voltage changes and parameter variation, while maintains the power quality of the DC microgrid. This means FOPID is less sensitive to variations of converter parameters than classical PID. Nevertheless, the FOPID implementation process is more complex because of its fractional order, but it can be approximated by using linear filters, in what is called as CRONE approximation.

On the other hand, the first-generation FOC is suitable for systems with gain variations and constant phase at the same frequency range. Despite not all converters have this kind of dynamic, the FOC offers a satisfactory performance and can be used in many power electronics systems.

7. Acknowledgment

This work is supported by the project entitled "*Low and medium capacity battery charger with low current THD, high power factor and high efficiency for electric vehicles*" sponsored by COLCIENCIAS, aims to support initiatives for the developing of novel technologies in the field of energy storage systems.

8. References

Alam, M.; Muttaqi, K.; Sutanto, D. (2013). Mitigation of rooftop solar PV impacts and evening peak support by managing the available capacity of distributed energy storage systems. *IEEE Transactions on Power Systems, 28*(4). https://doi.org/10.1109/TPWRS.2013.2259269

Banaei, Mohamad; Sani, Sajad (2018). Analysis and implementation of a new SEPIC-based single-switch buck-boost DC-DC converter with the continuous input current. *IEEE transactions on power electronics, 33*(12). https://doi.org/10.1109/TPEL.2018.2799876

Chun, Wang; Rui, Xiong; Hongwen, He; Xiaofeng, Ding; Weixiang, Shen (2016). Efficiency analysis of a bidirectional DC/DC converter in a hybrid energy storage system for plug-in hybrid electric vehicles. *Applied Energy, 183,* 612-622. https://doi.org/10.1016/j.apenergy.2016.08.178

Kanagaraj, N.; Al-Dhaifalla, M.; Nisar, K. S. (6-7 July 2017). Design of intelligent fuzzy fractional-order PID controller for pressure control application. *2017 International Conference on Intelligent Computing, Instrumentation and Control Technologies, ICICICT 2017*. https://doi.org/10.1109/ICICICT1.2017.8342618

Krishnamurthy, Vaidyanathan; Kwasinski, Alexis (2016). Effects of Power Electronics, Energy Storage, Power Distribution Architecture, and Lifeline Dependencies on Microgrid Resiliency during Extreme Events. *IEEE Journal of Emerging and Selected Topics in Power Electronics, 4*(4). https://doi.org/10.1109/JESTPE.2016.2598648

Kung, Sunny; Kish, Gregory (2018). A modular multilevel HVDC buck-boost converter delivered from its switched-mode counterpart. *IEEE Transactions on Power Delivery, 33*(1). https://doi.org/10.1109/TPWRD.2017.2690635

Lee, Soo; Kang, Yong; Park, Jung-Wook (2016). Optimal operation of multiple DGs in the DC distribution system to improve system efficiency. *IEEE Transactions on Industry Applications, 52*(5). https://doi.org/10.1109/TIA.2016.2582791

Lei, Yang; Xiong, Hejin; Lei, Deming (2-3 Dec. 2017). Fractional Order PID Control Strategy for Modular Multilevel Converters. *Proceedings - 2017 International Conference on Industrial Informatics - Computing Technology, Intelligent Technology, Industrial Information Integration, ICIICII 2017*. https://doi.org/10.1109/ICIICII.2017.21

Manandhar, Ujjal; Ukil, Abhisek; Jonathan, Tan (3-6 Nov. 2015). Efficiency comparison of DC and AC microgrid. In *Proceedings of the 2015 IEEE Innovative Smart Grid Technologies - Asia, ISGT ASIA 2015*. https://doi.org/10.1109/ISGT-Asia.2015.7387051

Montoya-Giraldo, Oscar; Garcés-Ruiz, Alejandro; Ortega-Velázquez, Isaac; Espinosa-Pérez, Gerardo (4-6 April 2018). Passivity-Based control for battery charging/discharging applications by using a buck-boost DC-DC converter. *2018 IEEE green technologies conference, GreenTech 2018*. https://doi.org/10.1109/GreenTech.2018.00025

Perez, G. A.; Kagan, N. (2016). *Integration of distributed generation in power distribution networks and its structure as an intelligent generation system*. https://doi.org/10.1109/ISGT-LA.2015.7568656

Sanchez-Choachi, Sebastián (2019). Control basado en pasividad con estrategia adaptativa de un sistema de almacenamiento energético para una nano-red DC. Re*vista Ingenierías Universidad de Medellín*, 18(35), 185-203.

Sirsi, Rohan; Prasad, Shashikant; Sonawane, Abhishek; Lokhande, Atul (7-8 April 2016). Efficiency comparison of AC distribution system and DC distribution system in a microgrid. En *International Conference on Energy Efficient Technologies for Sustainability, ICEETS 2016*. https://doi.org/10.1109/ICEETS.2016.7583774

Sun, HongGuang; Zhang, Yong; Baleanu, Dumitru; Chen, Wen; Chen, YangQuan (2018). A new collection of real-world applications of fractional calculus in science and engineering. *Communications in Nonlinear Science and Numerical Simulation, 64*, 213-231. https://doi.org/10.1016/j.cnsns.2018.04.019

Takagi, Masaaki; Iwafune, Yumiko; Yamaji, Kenji; Yamamoto, Hiromi; Okano, Kunihiko; Hiwatari, Ryoji; Ikeya, Tomohiko (2013). The economic value of PV energy storage using batteries of battery-switch stations. *IEEE Transactions on Sustainable Energy, 4*(1). https://doi.org/10.1109/TSTE.2012.2210571

Tamura, Shigeru (2016). Economic Analysis of Hybrid Battery Energy Storage Systems Applied to Frequency Control in Power System. *Electrical Engineering in Japan (English Translation of Denki Gakkai Ronbunshi), 195*(1). https://doi.org/10.1002/eej.22816

Tummuru, Narsa; Mishra, Mahesh; Srinivas, Srinivas (2015). Dynamic Energy Management of Renewable Grid Integrated Hybrid Energy Storage System. *IEEE Transactions on Industrial Electronics, 62*(12). https://doi.org/10.1109/TIE.2015.2455063